

COMPARISON BETWEEN SKY VIEW FACTOR VALUES
COMPUTED BY TWO DIFFERENT METHODS IN AN URBAN ENVIRONMENT

T. GÁL¹, M. RZEPA², B. GROMEK³ and J. UNGER¹

¹*Department of Climatology and Landscape Ecology, University of Szeged, P.O. Box 653, 6701 Szeged, Hungary
E-mail: tgal@geo.u-szeged.hu*

²*Department of Meteorology and Climatology, University of Lodz, Poland*

³*Department of Theoretical Physics, University of Lodz, Poland*

Összefoglalás – Munkánkban bemutatásra kerül az égbolthatóság (SVF) egy GIS alapú kiszámítási módja, ami egy városi 3D adatbázist alkalmaz. Ez a módszer lehetővé teszi egy város terület egészére kiterjedő folytonos SVF mező kiszámítását. Az ehhez hasonló városgeometriai adatbázisok elengedhetetlen kellékei a városi hőszigetel foglalkozó kutatásoknak. Munkánkban továbbá bemutatásra kerül egy terepi mérés is, ami az SVF halszem objektívvel készített fotókon alapuló kiértékeléséhez szükséges. Ez a fotografikus eljárás különösen alkalmas a városi környezethez és emellett elterjedt módja is az SVF meghatározásnak. A két módszer összevetése rámutat a kapott értékek eltérésére, amit többnyire a mérési pont körüli növényzettel magyarázhatunk. A növényzet hatásától eltekintve szignifikáns kapcsolat mutatható ki a két módszerrel számolt értékek között, ami alátámasztja a vektoros SVF számítási eljárás alkalmazásának lehetőségét városi környezetben. Ezzel a vektoros módszerrel (terepi mérések nélkül) egy folytonos SVF mező meghatározása egy teljes város területére csupán néhány napot vesz igénybe (aminek nagy része számítási idő), ha az épület adatbázis rendelkezésre áll. A vektoros számítási eljárás hibáját csökkenthetjük, ha felhasználunk a számítható városi növényzet adatbázisokat is.

Summary – In our study we present a GIS method for SVF calculation, which uses an urban 3D building database. This method provides opportunity to evaluate the continuous SVF field in an entire urbanized area. This kind of urban surface geometric database is essential for the researches on urban heat island. In this study we also present field measurements for the fish-eye photo based SVF calculation. This photographic technique is particularly well suited for urban environments and it is also a prevalent way of SVF determination. The comparison of the two methods shows that there are some differences – mostly caused by the presence of the vegetation around the measurement site – in the computed values. Apart from the vegetation there is significant correlation between the two values therefore the vector-based method can be considered capable of SVF calculation in an urban environment. With the vector-based method the calculation (without field measurements) of the continuous SVF field for an entire urban environment takes a few days (principally the computing time) if the building database is available. The error of the vector-based calculation can be decreased if a database of the intra-urban vegetation is applied.

Key words: urban environment, SVF calculations, 3D building database, fish-eye photographs, comparison

1. INTRODUCTION

Urban areas are an example of the most dramatic anthropogenic land use changes where primarily the geometry and surface characteristics have been, and are constantly being, altered. As a consequence, urban environments modify the energy and water balance which often results in higher urban temperature compared to the relatively natural surroundings (urban heat island – UHI). Different kinds of heat islands can be

distinguished: UHI under surface, on the surface, in the urban canopy layer (UCL) and in the urban boundary layer. The UHI is typically presented as a temperature difference between the air within the UCL (below the rooftops in the spaces between buildings) and that measured in a rural area outside the settlement (Oke, 1982). Generally, its strongest development occurs at night when the heat, stored in the daytime, is released (Landsberg, 1981; Oke, 1987).

Nocturnal cooling processes are primarily regulated by outgoing long wave radiation. In cities, narrow streets and high buildings create deep canyons. This 3D geometrical configuration plays an important role in regulating long-wave radiative heat loss, since due to the horizontal and vertical unevenness of the surface elements the outgoing long-wave radiation loss is more restricted here than in rural areas. Therefore, urban geometry is an important factor contributing to intra-urban temperature variations below roof level (e.g. Oke, 1981; Eliasson, 1996).

The sky view factor (SVF) is often used to describe urban geometry (e.g. Upmanis, 1999; Svensson, 2004). By definition, SVF is the ratio of the radiation received (or emitted) by a planar surface to the radiation emitted (or received) by the entire hemispheric environment (Watson and Johnson, 1987). It is a dimensionless measure between zero and one, representing totally obstructed and free spaces, respectively (Oke, 1988).

There are several techniques for the calculation of the SVF: using surveying techniques (e.g. Bottyán and Unger, 2003), digital camera with fish-eye lens (e.g. Grimmond et al., 2001; Chapman and Thornes, 2004; Rzepa and Gromek, 2006), signals from GPS receivers (Chapman et al., 2002; Chapman and Thornes, 2004) or more recently thermal fish-eye imagery (Chapman et al., 2007). The photographic technique is particularly well suited for urban environments, where buildings are variable in size and shape, and vegetation is present.

Modern 3D models describing the complex urban surface provide the opportunity of the GIS-based SVF evaluation. Among these software methods both raster- (e.g., Brown et al., 2001; Ratti et al., 2003; Lindberg, 2005) and vector-based approaches (e.g., Souza et al., 2003; Gulyás et al., 2006; Gál et al., 2007) are known.

The overall purpose of this study is to analyze the differences between SVF values computed with a vector-based algorithm (Gál et al., 2007) and with a photographic method, the so called BMSky-view (Rzepa and Gromek, 2006). The specific objectives are (i) to present and apply two different methods for SVF calculation in the same study area, (ii) to compare the two methods and analyze the difference between the values.

2. THE STUDY AREA AND THE 3D BUILDING DATABASE

Szeged (46°N, 20°E) is located in southeast Hungary, in the southern part of the Great Hungarian Plain at 79 m above sea level on a flat plain (Fig. 1). The region of Szeged belongs to the climatic type D.1 by Trewartha's classification which means continental climate with longer warm season (Unger, 1996). The urbanized area is around 30 km² within a larger administrative area (281 km²). Szeged is a medium-sized city among the Hungarian settlements with a population of about 160,000.

The creation of the applied 3D building database for Szeged was based on local municipality data of building footprints and aerial photos for the determination of individual building heights. The creation of the database is described in detail in Unger

(2006, 2007). For cross-checking, theodolite measurements were carried out and as a result, the mean ratio of the differences in the heights of the buildings was around 5%. The database covers the whole study area (27 km²) and consists of more than 22,000 buildings. Smaller, room-sized buildings are difficult to determine from the aerial photos, moreover their heat absorption and emission are negligible. Thus, buildings smaller than 15 m² were excluded from the database.

The measurement campaign for SVF determination in urban environment was carried out in a sample area of 0,41 km² in Szeged. There are various building types (with different footprint area and height) and density in this area thus it is suitable for the comparison of the values computed by the two different methods (*Fig. 1*).

To determine the elevation of the measurement points a Digital Elevation Model (DEM) is needed. This DEM for Szeged represents a bare surface with a small vertical variation of the surface (75.5–83 m a.s.l.). Both applied databases (elevation and building) use the Unified National Projection (EOV in Hungarian).

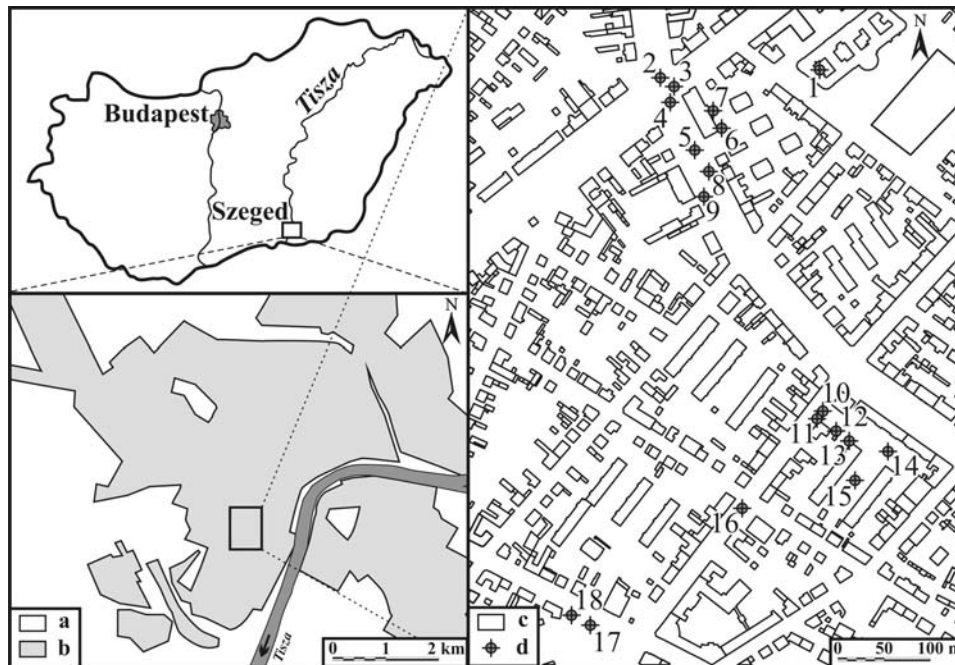


Fig. 1 The location of Szeged in Hungary and the location of the sample area in Szeged: (a) open area, (b) built-up area, (c) buildings (from the 3D building database) and (d) SVF measurement points

3. METHODS FOR THE SVF CALCULATIONS

As the main objective of our study is the comparison of the SVF values calculated from the 3D building database and from the fish-eye photographs, we selected 18 points in the sample area (*Fig. 1*). For these points SVF values were calculated with both methods resulting in two SVF values for each point:

- SVF_{vector} (computed by vector-based method from the 3D building database),

– $SVF_{\text{BMSky-View}}$ (computed by the BMSky-View algorithm from fish-eye photographs).

Before examining the differences it is necessary to present the fundamental characteristics of the two methods.

3.1. Algorithm for SVF_{vector} calculation using an urban vector database

The 3D building database of Szeged is a model of the real situation, which represents a simplified urban surface (containing buildings only). In this model all buildings have flat roof, and all walls of a building are of the same height.

The projection of every building on the sky is managed as the projection of their walls visible from a given surface point and polygon $g(x)$ is the border of the visible sky (Fig. 2a). After dividing the hemisphere equally into slices by rotation angle α , 'rectangles' are drawn whose heights are equal to the $g(x)$ values in the middle points of the intervals.

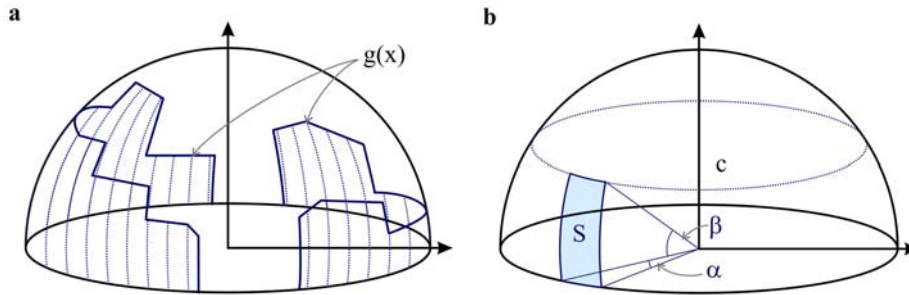


Fig. 2 (a) Polygon $g(x)$ as a border of the visible sky and dividing the hemisphere under $g(x)$ equally into slices by angle α (heights are equal to the $g(x)$ values in the middle points of the intervals), (b) a slice of a 'width' of α (S) of a basin with an elevation angle β

SVF values for a couple of common geometric arrangements are given by *Oke* (1987). In the case of the regular basin, where β is the elevation angle from the centre to the wall, the SVF value (referring to the centre) is: $SVF_{\text{basin}} = \cos^2\beta$. So the view factor (VF) of a basin with an elevation angle β is $VF_{\text{basin}} = 1 - \cos^2\beta = \sin^2\beta$, therefore the view factor for a slice (S) with a width of α (Fig. 2b) can be calculated as:

$$VF_S = \sin^2\beta \cdot (\alpha/360)$$

The algorithm draws a target line by the angle α from the selected point and along this line it searches the building which obstructs the largest part of the sky in that direction. The accuracy of the algorithm depends on the magnitude of the rotation angle (α). Smaller α angles result in a more accurate estimation of the SVF_{vector} but also mean longer computation time. After calculating the VF values by slices their sum is subtracted from 1 to get the SVF_{vector} .

For the automation of the process described above the ESRI ArcView 3.2 software (www.esri.com, 2006) is appropriate. It has a built-in object-oriented program language (Avenue). With the help of this language the software is programmable so that every element of the software is accessible (see also *Souza et al.*, 2003). Our application is compiled from 9 scripts (graphical surface, control of the parameters, calculation of SVF_{vector} , etc.). Fig. 3 illustrates the schematic description of the developed algorithm.

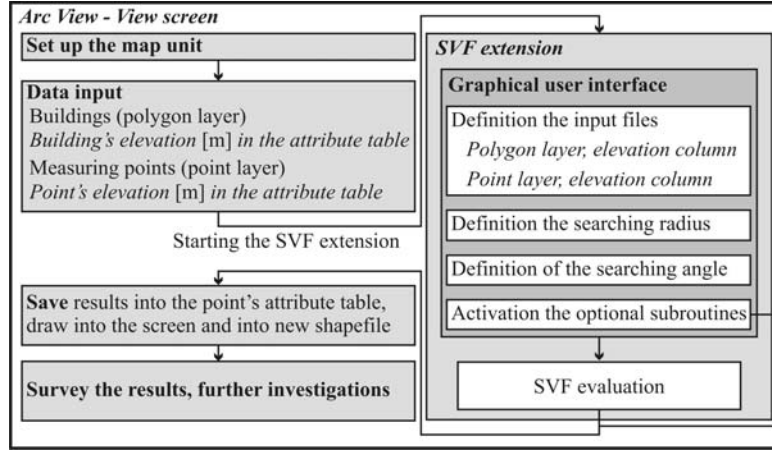


Fig. 3 Schematic description of the algorithm for the SVF_{vector} calculation using vector database

According to Fig. 3 values for two parameters have to be selected. These are (i) the radius of the area around the site where the algorithm takes the heights and positions of the buildings into consideration and (ii) the interval of the rotation angle (α) which determines the density of the target lines starting from the site. In our case a radius of 200 m and a rotation angle of 1° seemed to be appropriate (see more details in Unger, 2007).

3.2. Determining sky view factor using fish-eye photographs

BMSky-view is a user friendly application enabling to compute the SVF values directly from photos taken by digital camera with fish-eye lens.

This application works under Windows (Fig. 4). The algorithm of computing SVF was implemented using C++ programming language and based on a slight modification of the Steyn-method (Steyn, 1980). Steyn describes a method for determining the sky view factor from fish-eye lens photographs, which are divided into a number of concentric annuli of equal width, each representing an interval of zenith angles. Within each annulus he manually estimated the fraction of sky and derived the following formula:

$$SVF = \frac{1}{2 \cdot n} \sum_{i=1}^n \sin \left(\frac{\pi \left(i - \frac{1}{2} \right)}{2 \cdot n} \right) \cos \left(\frac{\pi \left(i - \frac{1}{2} \right)}{2 \cdot n} \right) \alpha_i$$

where α_i is the angular width of sky in the i -th annulus and n is the number of annuli (Barring et al., 1985).

3.3. Details of the field measurement and the application of the vector-based algorithm

For the determination of the $SVF_{\text{BMSky-View}}$ values photographs were taken with a camera equipped with fish-eye lens. We used a Nikon Coolpix 4300 camera with Nikon FC-E8 lens which is a prevalent tool for this application (e.g., Grimmond et al., 2001; Chapman and Thornes, 2004; Rzepa and Gromek, 2006). The fish-eye photographs were taken on 4 January 2006 therefore tree foliage was minimal. The camera was mounted to a

folding tripod and we recorded its height above the surface at each of the 18 selected points. At the same time we have located the points in a large-scale ortophoto-map (with a pixel resolution of 0.2 m). The $SVF_{\text{BMSky-View}}$ values were evaluated with the BMSky-view software from these fish-eye photographs.

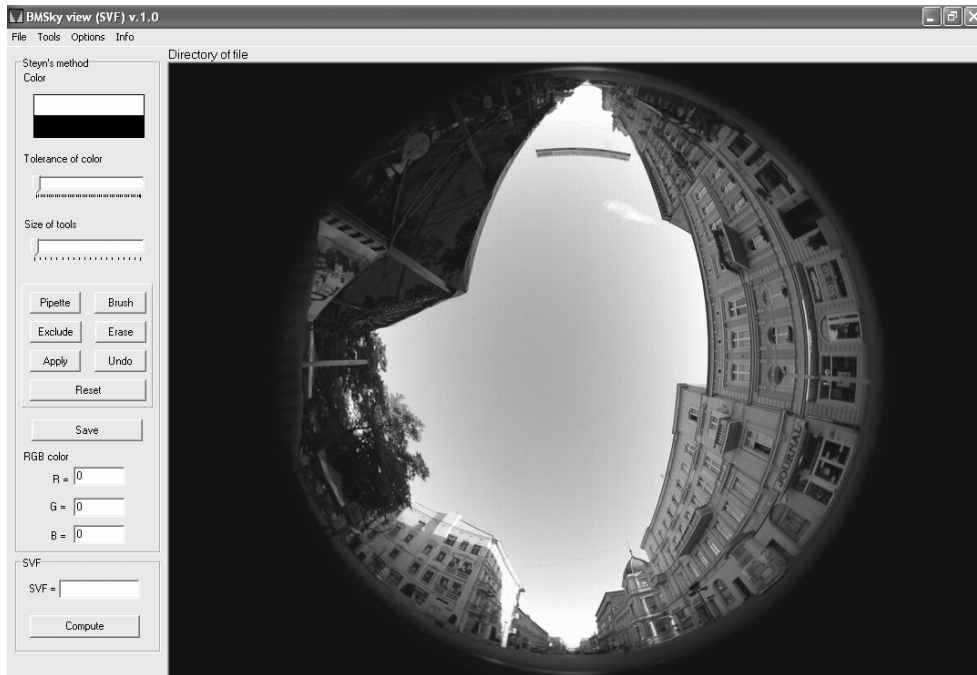


Fig. 4 Menu to recognize the sky area

The SVF_{vector} was determined in the same 18 points of the sample area with the vector-based algorithm. Using the ortophoto-map the horizontal coordinates of the measurement points (in the Unified National Projection) can be determined. For the determination of the accurate elevation of the points we took into account the heights of the camera above the surface and the elevation of the surface from a DEM covering the area.

4. DIFFERENCES BETWEEN THE SVF VALUES (EVALUATION AND EXPLANATION OF DIFFERENCES)

Firstly, we have compared visually the fish-eye photographs with the graphical results of the algorithm (Fig. 5). Based on this comparison we found minor deviations between the outlines of the buildings in the photos and the polygons, generated from the 3D building database with the SVF_{vector} algorithm.

The vegetation is not included in the database therefore the border of the sky in the presented photographs does not always coincide with the border generated by the algorithm. Apart from the vegetation there are other reasons that can cause some differences in the SVF values calculated by the two methods. For example there are traffic signs with relatively large sky obstruction (Fig. 5b).

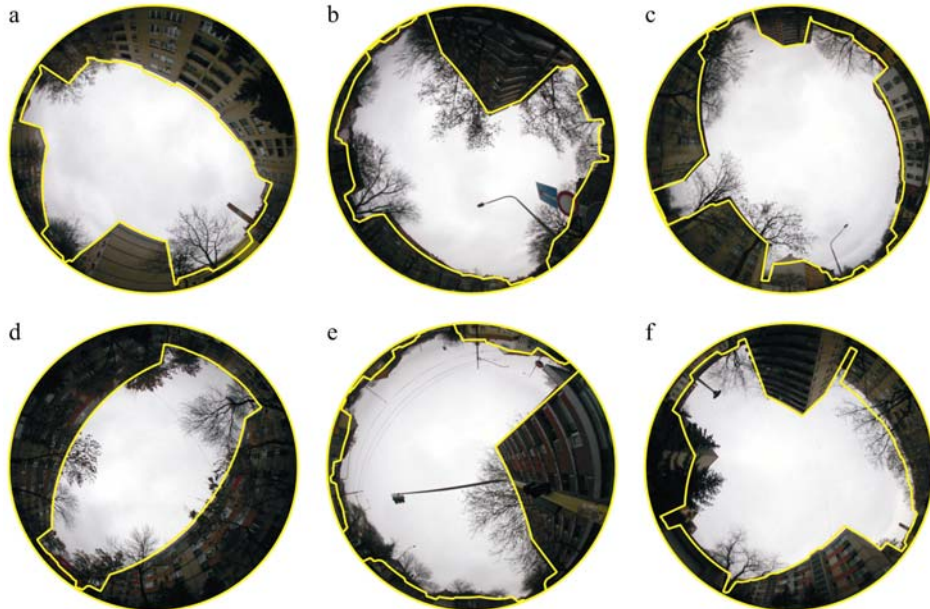


Fig. 5 Comparison of the fish-eye photographs and the graphical results of the SVF_{vector} algorithm in six selected points (point id: $a - 14$, $b - 5$, $c - 9$, $d - 15$, $e - 4$, $f - 12$)

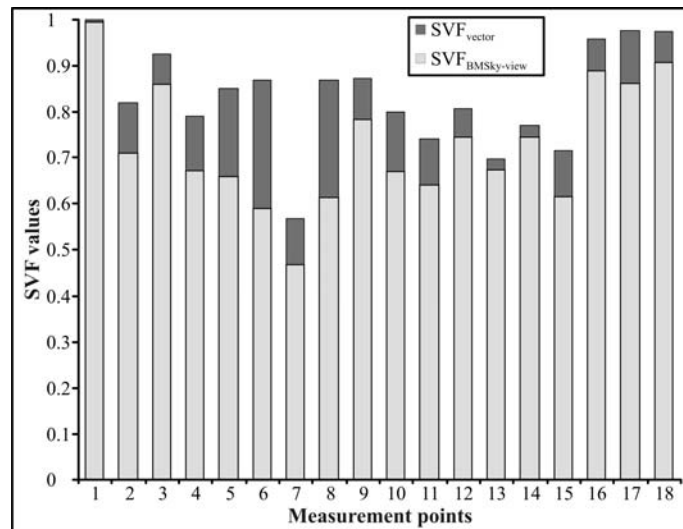


Fig. 6 Differences between the SVF_{vector} and $SVF_{BMSky-View}$ values at the 18 measurement points

The average difference between the $SVF_{BMSky-View}$ and the SVF_{vector} is 0.106 with the highest difference of 0.277. In the points where the vegetation is dense the $SVF_{BMSky-View}$ values are lower than the SVF_{vector} values (e.g. No. 4, 5, 15 in Fig. 5 and Fig. 6). If there is less vegetation the gap between the two values is decreasing (e.g. No. 14 in Fig. 5 and Fig. 6).

As the statistical comparison shows there is a relatively strong ($R^2 = 0.4452$) correlation between the SVF values if we use the linear $y = ax$ formula (Fig. 7). If the constant is included in the equation ($y = ax + b$) we get a closer connection ($R^2 = 0.7038$) and the constant (b) is 0.3176 in this case. The inclusion and the magnitude of the constant can be explained by the effect of the vegetation. Both coefficients of determination (R^2) are significant at the 1% level, however we have to note that these relationships are valid only for the range of the SVF values of our case (0.46 – 1).

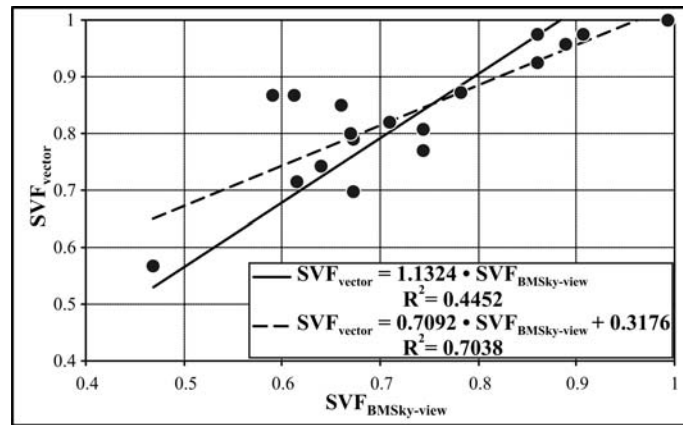


Fig. 7 Relationship between the SVF values calculated by the applied methods in the sample area (n = 18)

5. CONCLUSIONS

The derivation of a continuous image of SVF covering large urban areas is necessary to study the relationship between urban geometry quantified by SVF and intra-urban nocturnal temperature variations. It means thousands of SVF calculations in the selected urban area (Unger, 2007; Gál et al., 2007). Only GIS-based methods are suitable for this kind of evaluation. In our study we presented a GIS method for the SVF calculation which uses an urban 3D building database.

Before the application of this continuous SVF field for studying its relationship with the urban heat island field we had to check the errors of this method. The photographic technique is particularly well suited for urban environments and it is also a prevalent way of SVF determination. Thus the SVF values from one of the photographic methods (BMSky-view) are suitable for studying the errors of the vector-based method. In this study we presented field measurements to take fish-eye photographs and we applied the above-mentioned SVF calculation method based on these photos.

The comparison of the two methods showed that there are some differences between the obtained values. These differences are caused mainly by the presence of vegetation around the measurement sites. Apart from the vegetation there is a close connection between the values therefore the vector-based method is appropriate for the SVF calculation in urban environment.

With the vector-based method the calculation (without field measurements) of the continuous SFV field for an entire urban environment takes a few days if the building database is available. Applying a database of the intra-urban vegetation the error of the vector-based calculation could be decreased.

Acknowledgements – This research was supported by the grant of the Hungarian Scientific Research Fund (OTKA T/049573 and K-67626).

REFERENCES

- Bähring, L., Mattsson, J.O. and Lindqvist, S., 1985: Canyon geometry, street temperatures and urban heat island in Malmö, Sweden. *J. Climatol.* 5, 433-444.
- Bottyán, Z. and Unger, J., 2003: A multiple linear statistical model for estimating the mean maximum urban heat island. *Theor. Appl. Climatol.* 75, 233-243.
- Brown, M.J., Grimmond, C.S.B. and Ratti, C., 2001: Comparison of methodologies for computing sky view factor in urban environment. *International Society of Environmental Hydraulics Conference*, Tempe, AZ. *Internal Report Los Alamos National Laboratory*, Los Alamos, NM. LA-UR-01-4107.
- Chapman, L. and Thornes, J.E., 2004: Real-time sky-view factor calculation and approximation. *J. Atmos. Oceanic. Technol.* 21, 730-742.
- Chapman, L., Thornes, J.E. and Bradley, A.V., 2002: Sky-view factor approximation using GPS receivers. *Int. J. Climatol.* 22, 615-621.
- Chapman, L., Thornes, J.E., Muller, J-P. and McMurdoch, S., 2007: Potential applications of thermal fisheye imagery in urban environments. *IEEE Geoscience and Rem. Sens. Letters* 4, 56-59.
- Eliasson, I., 1996: Urban nocturnal temperatures, street geometry and land use. *Atmos. Environ.* 30, 379-392.
- Gál, T., Lindberg, H.E. and Unger, J., 2007: Computing continuous sky view factor using 3D urban raster and vector databases: comparison and an application for urban climate. *Theor. Appl. Climatol.* (in press)
- Grimmond, C.S.B., Potter, S.K., Zutter, H.N., and Souch, C., 2001: Rapid methods to estimate sky-view factors applied to urban areas. *Int. J. Climatol.* 21, 903-913.
- Gulyás, Á., Unger, J. and Matzarakis, A., 2006: Assessment of the microclimatic and human comfort conditions in a complex urban environment: modelling and measurements. *Building and Environment* 41, 1713-1722.
- Landsberg, H.E., 1981: *The urban climate*. Academic Press, New York.
- Lindberg, F., 2005: Towards the use of local governmental 3-D data within urban climatology studies. *Mapping and Image Science* 2, 32-37.
- Oke, T.R., 1981: Canyon geometry and the nocturnal urban heat island: comparison of scale model and field observations. *J. Climatol.* 1, 237-254.
- Oke, T.R., 1982: The energetic basis of the urban heat island. *Quart. J. Roy. Meteorol. Soc.* 108, 1-24.
- Oke, T.R., 1987: *Boundary layer climates*, Routledge, London and New York.
- Oke, T.R., 1988: Street design and urban canopy layer climate. *Energy and Buildings* 11, 103-113.
- Ratti, C., Raydan, D. and Steemers, K., 2003: Building form and environmental performance: archetypes, analysis and an arid climate. *Energy and Buildings* 35, 49-59.
- Rzepa, M. and Gromek, B., 2006: Variability of sky view factor in the main street canyon in the center of Łódź. *Preprints Sixth Int. Conf. on Urban Climate*, Göteborg, Sweden. 854-857.
- Souza, L.C.L., Rodrigues, D.S. and Mendes, J.F.G., 2003: The 3D SkyView extension: an urban geometry access tool in a geographical information system. In Klyzik, K., Oke, T.R., Fortuniak, K., Grimmond, C.S.B. and Wibig, J. (eds.): *Proceed Fifth Int Conf on Urban Climate*. Vol. 2. University of Lodz, Lodz, Poland. 413-416.
- Steyn, D.G., 1980: The calculation of view factors from fish-eye lens photographs. *Atmosphere-Ocean* 18, 254-258.
- Svensson, M., 2004: Sky view factor analysis – implications for urban air temperature differences. *Meteorol. Applications* 11, 201-211.
- Unger, J., 1996: Heat island intensity with different meteorological conditions in a medium-sized town: Szeged, Hungary. *Theor. Appl. Climatol.* 54, 147-151.
- Unger, J., 2006: Modelling of the annual mean maximum urban heat island with the application of 2 and 3D surface parameters. *Clim. Res.* 30, 215-226.

Tamas Gál, Marcin Rzepa, Bartosz Gromek and János Unger

Unger, J., 2007: Connection between urban heat island and sky view factor approximated by a software tool on a 3D urban database. Int. J. Environ. and Pollution (in press)

Upmanis, H., 1999: The influence of sky view factor and land use on city temperatures. In Upmanis, H.: Influence of Parks on Local Climate. Earth Sciences Centre, Göteborg University A 43, paper 3.

www.esri.com, 2006